

Effect of a Triaxial Nuclear Shape on Proton Tunneling: The Decay and Structure of ^{145}Tm

D. Seweryniak,¹ B. Blank,^{1,2} M. P. Carpenter,¹ C. N. Davids,¹ T. Davinson,³ S. J. Freeman,⁴ N. Hammond,¹ N. Hoteling,⁵ R. V. F. Janssens,¹ T. L. Khoo,¹ Z. Liu,³ G. Mukherjee,¹ A. Robinson,³ C. Scholey,⁶ S. Sinha,¹ J. Shergur,⁵ K. Starosta,⁷ W. B. Walters,⁵ A. Woehr,⁸ and P. J. Woods³

¹Argonne National Laboratory, Argonne, Illinois 60439, USA

²Centre d'Etudes Nucleaires de Bordeaux-Gradignan, F-33175 Gradignan Cedex, France

³University of Edinburgh, Edinburgh EH9 3JZ, United Kingdom

⁴University of Manchester, Manchester M13 9PL, United Kingdom

⁵University of Maryland, College Park, Maryland 20742, USA

⁶University of Jyväskylä, Jyväskylä, Finland

⁷National Superconducting Cyclotron Laboratory, East Lansing, Michigan 48824, USA

⁸University of Notre Dame, Notre Dame, Indiana 46556, USA

(Received 24 July 2006; published 24 August 2007)

Gamma rays deexciting states in the proton emitter ^{145}Tm were observed using the recoil-decay tagging method. The ^{145}Tm ground-state rotational band was found to exhibit the properties expected for an $h_{11/2}$ proton decoupled band. In addition, coincidences between protons feeding the 2^+ state in ^{144}Er and the $2^+ \rightarrow 0^+$ γ -ray transition were detected, the first measurement of this kind, leading to a more precise value for the 2^+ excitation energy of 329(1) keV. Calculations with the particle-rotor model and the core quasiparticle coupling model indicate that the properties of the $\pi h_{11/2}$ band and the proton-decay rates in ^{145}Tm are consistent with the presence of triaxiality with an asymmetry parameter $\gamma \approx 20^\circ$.

DOI: [10.1103/PhysRevLett.99.082502](https://doi.org/10.1103/PhysRevLett.99.082502)

PACS numbers: 23.20.Lv, 23.50.+z, 27.60.+j

Most nuclei are axially symmetric. However, specific combinations of single-particle orbitals near the Fermi surface can lead to a propensity towards triaxial shapes as illustrated by recent calculations of the gain in the total nuclear binding energy due to nonaxial degrees of freedom [1], which revealed several “islands” of triaxiality throughout the nuclidic chart. One of the islands corresponds to the $N = 76, 77, 78$ isotones above the $Z = 50$ proton shell in the vicinity of the proton drip line, near the ^{145}Tm proton emitter. This offers a unique opportunity to study proton tunneling through a 3-dimensional Coulomb barrier. Conversely, the proton emission can be used as a probe of triaxial shapes.

In recent years, studies of proton emitters have become a source of detailed nuclear structure information beyond the proton dripline. The anomalous proton-decay rates in the ^{131}Eu and ^{141}Ho proton emitters were associated with large prolate deformation [2]. In fact, it was proposed that the transition from spherical to deformed shapes in this region of nuclei is responsible for a sudden change in the “intrinsic” proton-decay rate [3]. The observation of rotational bands feeding the ground state and an isomeric state in ^{141}Ho combined with its proton-decay properties provided constraints on the departure from axial symmetry in this nucleus [4]. The three known proton emitting Tm isotopes, $^{147,146,145}\text{Tm}$, are located between spherical nuclides close to the $N = 82$ major shell closure and an island of large prolate deformation to which ^{131}Eu and ^{141}Ho belong. The microscopic-macroscopic calculations of Möller *et al.* [5] predict a prolate quadrupole deformation of $\beta_2 = 0.25$ for the ^{145}Tm nucleus. The heavier Tm isotopes, ^{146}Tm and

^{147}Tm , are calculated to have an oblate shape with $\beta_2 = -0.20$ and $\beta_2 = -0.19$, respectively. The transition between oblate and prolate shapes is another manifestation of the softness towards triaxial shapes.

Proton emission from the ^{145}Tm ground state was observed for the first time in Ref. [6], where a proton energy of $E_p = 1728(10)$ keV and a half-life of $T_{1/2} = 3.5(10)$ μs were reported. In a follow-up measurement [7], a $b_p = 9.6(1.5)\%$ proton-decay branch to the 2^+ excited state in the daughter nucleus ^{144}Er was observed and a more precise half-life of 3.1(3) μs was determined. The 2^+ excitation energy in the daughter nucleus, $E(2^+) = 330(10)$ keV, was deduced from the energy difference between the two proton lines.

The cross section for producing ^{145}Tm in a fusion-evaporation reaction is of the order of 100 nb and tens of other nuclei with a total cross section approaching 1 b are populated at the same time. Thus, an efficient and very selective detection technique is required. A 417-MeV ^{92}Mo beam from the ATLAS accelerator facility at Argonne National Laboratory impinged on a 0.6 mg/cm² thick, highly enriched, ^{58}Ni target to populate ^{145}Tm nuclei after evaporation of 1 proton and 4 neutrons. The average beam intensity was about 5 pA for a period of about 90 h. The recoil-decay tagging method [8] was used to select γ rays in ^{145}Tm . Prompt γ radiation was detected in the Gammasphere array of 90 Compton suppressed HPGe detectors which surrounded the target [9,10]. Recoiling nuclei were separated from the beam and dispersed according to their mass-to-charge state ratio in the Argonne Fragment Mass Analyzer [11]. Only residues with mass

145 and charge states 25^+ and 26^+ were implanted into a double-sided silicon strip detector (DSSD). The front and back side of the $32 \times 32 \text{ mm}^2$, $60 \text{ }\mu\text{m}$ -thick, DSSD were divided into 80 orthogonal strips each. Following the implantation, the recoils decayed in the pixel where they were implanted. Using spatial and time correlations, the decays were associated with individual implants. In addition, a 55% HPGe detector was placed behind the DSSD to enable proton- γ coincidence measurements.

The proton energy spectrum measured within $250 \text{ }\mu\text{s}$ of the implantation is shown in Fig. 1. The spectrum is dominated by the proton line with an energy of $E_p = 1720(10) \text{ keV}$ and a half-life of $T_{1/2} = 3.17(20) \text{ }\mu\text{s}$ corresponding to the ^{145}Tm ground-state-to-ground-state proton decay, in agreement with the previous measurement [7]. The two weak lines in Fig. 1 correspond to the ^{145}Tm ground-state decay to the 2^+ level in the ^{144}Er daughter and to the known proton decay from the isomer in ^{141}Ho [12], respectively. A branching ratio of 10.4(21)% was deduced for the ^{145}Tm proton decay to the 2^+ state, which agrees with the previously reported value [7].

The inset of Fig. 1 contains a coincidence matrix between decay events measured in the DSSD and γ rays detected in the HPGe placed behind the DSSD. Six out of the total of seven events in this matrix have proton energies corresponding to the low-energy, weak ^{145}Tm proton line. The γ -ray energies of two events are identical and equal to 329 keV. These were interpreted as full-energy photopeak events. The energies of the remaining events are spread between 100 and 300 keV and are due to Compton scattering in the HPGe detector. Therefore, the data are consistent with coincidences between protons feeding the 2^+ state and the $2^+ \rightarrow 0^+$ γ -ray transition in the ^{144}Er daughter nucleus. This measurement constitutes the first observation of proton- γ coincidences in a ground-state proton emitter and was achieved despite a cross section

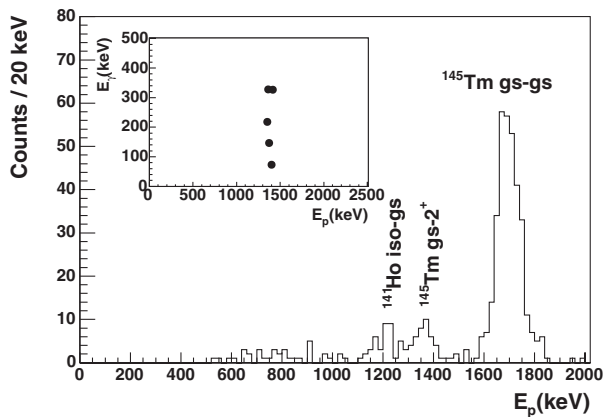


FIG. 1. The spectrum of protons detected within $250 \text{ }\mu\text{s}$ after recoil implantation in the DSSD. The coincidence matrix between protons and γ rays is shown in the inset (see text for details).

of only about 10 nb for the fine structure decay. The deduced 2^+ excitation energy of 329(1) keV agrees with the value of 330(10) keV obtained previously [7], but is more precise.

The spectrum of γ rays correlated with the ^{145}Tm ground-state-to-ground-state proton decay is presented in Fig. 2(a). A regular sequence of three γ rays with energies 338, 530, and 686 keV can be seen in the spectrum. These three transitions are in coincidence with each other, as illustrated by the 686-keV coincidence gate shown in Fig. 2(b) and the sum of the 338, 530, 686 keV gates in Fig. 2(c). Two weaker lines at 819 and 938 keV can also be seen in Fig. 2. Based on the energies of these transitions it is proposed that they form a $\pi h_{11/2}$ decoupled rotational band (see discussion below). A closer inspection reveals the presence of 3 additional weak transitions with energies 478, 806, and 927 keV. Because of the low coincidence statistics they were not placed in the level scheme. The energies and intensities of the γ rays assigned to ^{145}Tm are included in Table I. The proposed ^{145}Tm decay level scheme is presented in Fig. 3.

The proton $h_{11/2}$ intruder orbital is located close to the Fermi surface in the proton-rich $A \approx 130\text{--}150$ nuclei. Deformed, proton-rich, odd- Z nuclei in this mass region

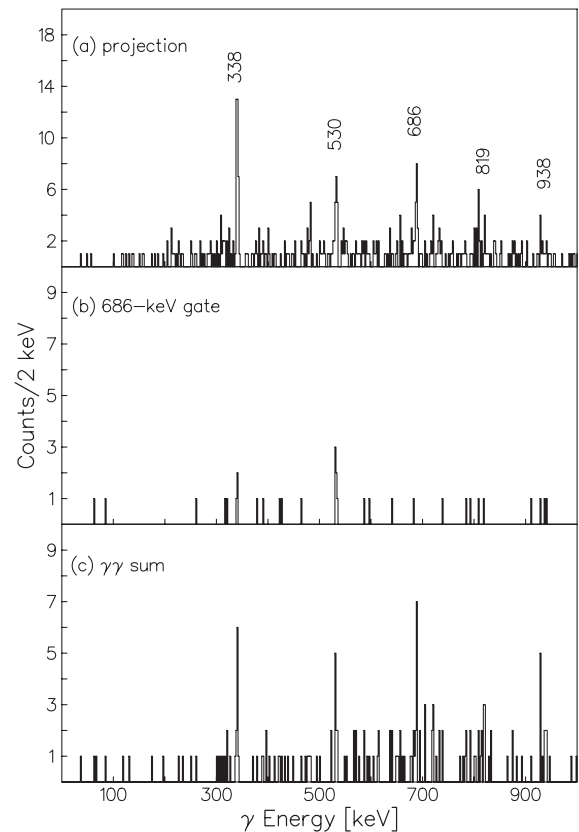
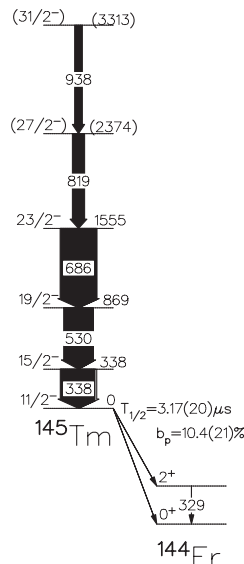


FIG. 2. (a) The γ spectrum tagged with the ^{145}Tm protons. (b) The 686-keV coincidence gate. (c) The sum of the 338, 530, and 686 keV coincidence gates.

TABLE I. Gamma-ray transitions in ^{145}Tm observed in the $^{58}\text{Ni}(417\text{ MeV}) + ^{92}\text{Mo}$ reaction.

| γ energy | γ intensity | γ assignment |
|-----------------|--------------------|-------------------------------|
| 338.4(4) | 100(18) | $15/2^- \rightarrow 11/2^-$ |
| 478.1(10) | 38(14) | |
| 530.4(5) | 84(19) | $19/2^- \rightarrow 15/2^-$ |
| 686.2(5) | 105(25) | $23/2^- \rightarrow 19/2^-$ |
| 805.9(8) | 78(28) | |
| 818.8(7) | 35(21) | $(27/2^- \rightarrow 23/2^-)$ |
| 926.8(7) | 36(22) | |
| 937.7(8) | 22(15) | $(31/2^- \rightarrow 27/2^-)$ |

exhibit strongly populated rotational bands based on this $\pi h_{11/2}$ state. A combination of moderate deformation and high single-particle angular momentum, $j = 11/2$, results in a relatively strong Coriolis interaction, which manifests itself already at low spin. This leads to the decoupling of the $h_{11/2}$ proton from the core and to the alignment of the proton angular momentum along the angular momentum of the core. As a result, a decoupled band is formed with level energies: $E(11/2^-)$, $E(15/2^-)$, \dots , similar to those of the ground-state rotational band in the even-even core: $E(0^+)$, $E(2^+)$, \dots [13]. The systematics of proton $h_{11/2}$ decoupled bands and ground-state bands in even-even, proton-rich rare-earth nuclei is presented in Figs. 4(a) and 4(b), respectively. The γ -ray energies in the odd-Z nuclei and their even-even cores are indeed similar. The energies of the transitions assigned to the ^{145}Tm ground-state band agree very well with the systematics of the proton $h_{11/2}$ decoupled bands. The energy of the bottom transition is 338 keV, very close to the energy of the 2^+ state in the even-even core of 329 keV measured in this work. Consequently, it is proposed here that the observed

FIG. 3. The proposed level scheme for ^{145}Tm .

sequence of γ rays in ^{145}Tm forms a decoupled $\pi h_{11/2}$ band. It is instructive to study the behavior of the $E(19/2^-)/E(15/2^-)$ and $E(4^+)/E(2^+)$ energy ratios [see Figs. 4(c) and 4(d)]. For $N = 78$ isotones, the ratio is about 2.3, just above the 2.0 value corresponding to a harmonic vibrator and below the 2.5 value characteristic of a γ soft rotor (or a triaxial rigid rotor, with an asymmetry parameter $\gamma \approx 30^\circ$). At $N = 76$, where ^{145}Tm is situated, this ratio is almost exactly 2.5 and it increases to about 2.7 for the $N = 74$ isotones.

The changes in the moment of inertia, $J_1/\hbar^2 = \frac{1}{2} \times [dE/d(I-j)^2]^{-1}$, where E, I are the level energy and spin and j is the odd proton angular momentum, as a function of the rotational frequency, $\hbar\omega = dE/d(I-j)$, are compared with the results of particle-rotor calculations in Fig. 5. A Woods-Saxon potential, with the universal set of parameters [14], was used in the calculations. The proton pairing strength was set to $G_p = 0.136\text{ MeV}$, and the Coriolis interaction was attenuated by 15%. The moment of inertia was adjusted to fit the $E(2^+)$ energy of the core. When the measured $E(2^+)$ energy of the ^{144}Er core is used, the best agreement between calculations and experiment for states with spin between $11/2$ and $23/2$ was obtained for $\gamma \approx 30^\circ$, for both $\beta_2 = 0.18$ and 0.25 . When the $E(2^+)$ energy is decreased to 210 keV in order to account for the increase of the moment of inertia similar to the $N = 76$ isotone ^{142}Dy (see Fig. 5) $\gamma \approx 20^\circ$ fits the data very well.

The particle-vibrator proton-decay rate calculations reported good agreement with the experiment using a dynamical deformation of $\beta_2 = 0.18$ [7,15]. According to these calculations the $\pi h_{11/2} \otimes 0^+$ and $\pi f_{7/2} \otimes 2^+$ components of the ^{145}Tm ground state are responsible for the decay to the 0^+ ground state and to the 2^+ excited state,

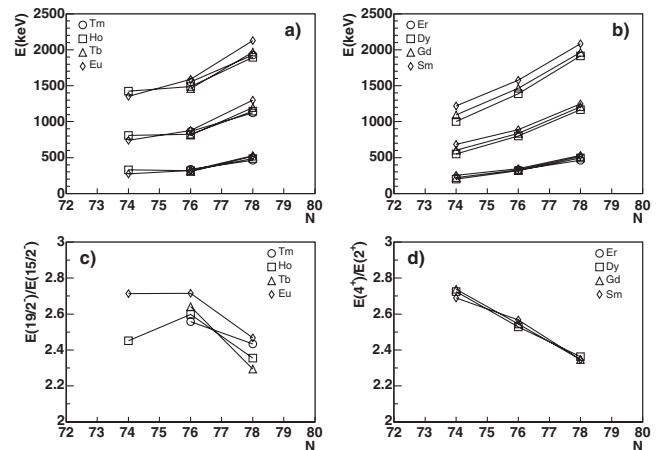


FIG. 4. The energies of (a) the $15/2^-$, $19/2^-$, $23/2^-$ states (relative to the $11/2^-$ state) and (b) the 2^+ , 4^+ , 6^+ states (relative to the 0^+ state) in the proton-rich rare-earth nuclei. The energy ratios for (c) the $15/2^-$ and $19/2^-$ states and for (d) the 4^+ and 2^+ states.

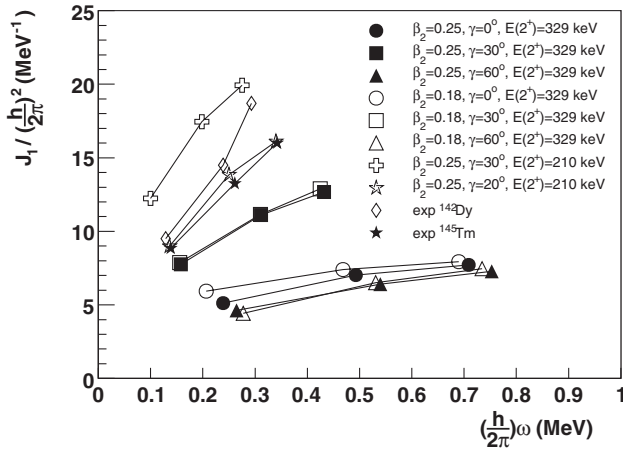


FIG. 5. The moment of inertia as a function of the rotational frequency extracted for the ^{145}Tm $\pi h_{11/2}$ band and the values calculated with the particle-rotor model using different quadrupole deformations (β_2), asymmetry parameters (γ), and moments of inertia (see text for details). The moment of inertia for the even-even $N = 76$ isotope ^{142}Dy is also plotted.

respectively. In order to obtain the ^{145}Tm ground-state wave function, calculations using the core quasiparticle coupling model (CQPCM) were performed [16]. The particle-core coupling constant was adjusted to reproduce level energies of the $\pi h_{11/2}$ band in ^{141}Eu [17]. For $\beta_2 = 0.18$, amplitudes of 57% and 2.7% were calculated for the two components above, respectively, which compares well with particle-vibrator calculations: (33%, 4.0%) [15] and (56%, 3.0%) [7]. Adding nonzero γ values worsens this agreement. However, using deformations $\beta_2 = 0.25$ and $\gamma = 25^\circ$ results in a similar wave function, namely, (50%, 2.7%). Thus, triaxiality appears to be consistent with the excited states and decay properties of ^{145}Tm .

The ^{145}Tm proton decay is very complex from a theoretical point of view. First, the existence of a decoupled band suggests that the Coriolis force dominates the ^{145}Tm structure. Second, as indicated above, ^{145}Tm could be triaxial. The so-called adiabatic proton-decay models neglect the Coriolis force [18]. On the other hand, nonadiabatic models, which include the Coriolis interaction, did not reproduce proton-decay data for the deformed proton emitter ^{141}Ho [18,19]. In Ref. [20], this discrepancy was eliminated by using the quasiparticle description, which attenuates the Coriolis matrix elements through pairing. Nonaxial degrees of freedom were included in the adiabatic [21] and nonadiabatic [22] approach, but pairing was not. In order to describe in detail the ^{145}Tm proton decay both the Coriolis force in the quasiparticle formulation together with nonaxial shapes should be included.

In summary, the ground-state band in the proton emitter ^{145}Tm was observed. In addition, coincidences between the protons feeding the 2^+ state and the $2^+ \rightarrow 0^+$ γ -ray transition in the daughter nucleus were detected. The ^{145}Tm ground-state band has properties characteristic of a proton $h_{11/2}$ decoupled band. The comparison between the particle-rotor model and the measured level energies suggests that an asymmetry parameter $\gamma \approx 20^\circ$ fits the data best. The CQPCM indicates that $\beta_2 = 0.25$ and $\gamma \approx 25^\circ$ are consistent with both the ^{145}Tm proton-decay rates and the spectrum of excited states.

This work was supported by the U.S. Department of Energy, Office of Nuclear Physics, under Contracts No. DE-AC02-06CH11357 and No. DE-FG02-94-ER49834.

-
- [1] P. Möller *et al.*, Phys. Rev. Lett. **97**, 162502 (2006).
 - [2] C. N. Davids *et al.*, Phys. Rev. Lett. **80**, 1849 (1998).
 - [3] D. S. Delion, R. J. Liotta, and R. Wyss, Phys. Rev. Lett. **96**, 072501 (2006).
 - [4] D. Seweryniak *et al.*, Phys. Rev. Lett. **86**, 1458 (2001).
 - [5] P. Möller *et al.*, At. Data Nucl. Data Tables **59**, 185 (1995).
 - [6] J. C. Batchelder *et al.*, Phys. Rev. C **57**, R1042 (1998).
 - [7] M. Karny *et al.*, Phys. Rev. Lett. **90**, 012502 (2003).
 - [8] E. S. Paul *et al.*, Phys. Rev. C **51**, 78 (1995).
 - [9] I. Y. Lee, Nucl. Phys. **A520**, c641 (1990).
 - [10] R. V. F. Janssens and F. S. Stephens, Nucl. Phys. News **6**, 9 (1996).
 - [11] C. N. Davids *et al.*, Nucl. Instrum. Methods Phys. Res., Sect. B **70**, 358 (1992).
 - [12] K. Rykaczewski *et al.*, Phys. Rev. C **60**, 011301(R) (1999).
 - [13] F. S. Stephens, Rev. Mod. Phys. **47**, 43 (1975).
 - [14] J. Dudek, Z. Szymański, and T. Werner, Phys. Rev. C **23**, 920 (1981).
 - [15] C. N. Davids and H. Esbensen, Phys. Rev. C **64**, 034317 (2001).
 - [16] A. Klein, Phys. Rev. C **63**, 014316 (2000).
 - [17] N. Xu *et al.*, Phys. Rev. C **43**, 2189 (1991).
 - [18] H. Esbensen and C. N. Davids, Phys. Rev. C **63**, 014315 (2000).
 - [19] A. T. Kruppa, B. Barmore, W. Nazarewicz, and T. Vertse, Phys. Rev. Lett. **84**, 4549 (2000).
 - [20] G. Fiorin, E. Maglione, and L. S. Ferreira, Phys. Rev. C **67**, 054302 (2003).
 - [21] C. N. Davids and H. Esbensen, Phys. Rev. C **69**, 034314 (2004).
 - [22] A. T. Kruppa and W. Nazarewicz, Phys. Rev. C **69**, 054311 (2004).